Discover Chemistry

RESEARCH Open Access

Characterization of silver nanoparticles synthesized from *Helianthus annuus* leaf extracts and antibacterial potential against foodborne pathogens

Racheal O. Fashogbon[1*], Olubunmi P. Adejoh[2], Samuel A. Fasiku[1], Stephanie N. James[1], Olutosin O. Ajayi[1] and Abiodun A. Adeyemi[3]

*Correspondence:
Racheal O. Fashogbon
ro.fashogbon@acu.edu.ng
[1]Department of Microbiology and Biotechnology, Faculty of Natural Sciences, Ajayi Crowther University, Oyo, Nigeria
[2]Microbiology Research Section, Patent and Enterprise Incubation Centre, Forestry Research Institute of Nigeria, Jericho Hill, Ibadan, Nigeria
[3]Department of Pharmacognosy and Herbal Medicine, Faculty of Pharmacy, University of Ibadan, Ibadan, Nigeria

Abstract
The synthesis of nanoparticles using biological substances, such as plants, has proven to be more beneficial, eco-friendly, and cost-effective. This study emphasised the green biogenic synthesis of silver nanoparticles (AgNPs) from *Helianthus annuus* L. leaf extracts in ethyl acetate (AgNPEa) and methanol (AgNPM), along with antibacterial and antioxidant properties of the resulting nanoparticles. The phytochemical analysis of the ethanol and ethyl acetate extracts was done. Characterization (UV-visible (UV-Vis), Fourier transform infrared (FT-IR), energy dispersive X-ray (EDX), scanning electron microscopy (SEM), X-ray diffraction techniques (XRD) and FTIR), antioxidant and antibacterial potential of the synthesised AgNPs were done. The two extracts showed no cardiac glycosides. A change in colour of the silver salt solution, showing a maximum UV-vis absorbance at 450 nm for AgNPMHa and 500 nm for AgNPEaHa. The SEM and TEM revealed a spherical shape having about 26.8 ± 9.4 nm and 22.3 ± 6.8 nm size. The EDX showed a high silver content of 69.35% in AgNPMHa and 72.40% in AgNPEaHa while XRD showed planes of pure silver ions. FTIR analysis the capping and stabilization of nanoparticle. Hydrogen peroxide, reducing power and total antioxidant activity increased dose-dependently (55 ± 23%, 63%, and 57% for AgNPEaHa and 57.03 ± 17%, 69.62 ± 21%, and 56% for AgNPMHa at 400ul) and both susceptible to *Escherichia coli*. The results confirmed that *Helianthus annuus* is a potential biomaterial for synthesizing AgNPs which can be exploited for its antioxidant and antibacterial activity.

Keywords Antioxidant assay, Antibacterial activity, *Helianthus annuus*, Phytochemicals and nanoparticles

1 Introduction

Recently, the field of nanotechnology has become one of the most effective areas in research with extended biological systems for producing modern nanoscale materials. Nanotechnology has been utilised extensively in various disciplines, including biology,

medicine, physics, chemistry, and material sciences. It is being applied to tissue engineering, drug delivery, and biosensor manufacturing in the biomedical domains [1]. Formation of nanoparticles using extracts from plants, microorganisms, and enzymes has been more beneficial than physical and chemical methods because it is not expensive, eco-friendly, and effortlessly amplified for large-scale processes [2].

Phytonanotherapy combines the benefits of plants with metal nanoparticles that mimic the effects of pharmaceutical medications but with fewer adverse effects [3]. Silver is one of the metals that is most promising for use in the creation of nanoparticles since it is highly poisonous to microorganisms and has very little effect on mammals. Several ointments and lotions contain silver, which serves as an antibacterial agent to stop burns and wound infections [4]. Leaf extracts are used to create silver nanoparticles (AgNPs) and have demonstrated antibacterial efficacy against hosts of microbial infections [5]. They were found to be the origin of Ag^{+} ions by integrating into bacterial proteins, causing cell membranes to become depleted [6, 7]. This biosynthesis-based strategy is appealing because cell-free biomolecular extracts containing free amino acids and organic acids might be used to extracellularly synthesise AgNPs. Apart from the antimicrobial potential of phytonanoparticles, the antioxidant capacity is highly recognised. In oxygen-dependent (aerobic) biological systems, free radicals are essential for breathing and other vital cellular functions, but they also contribute to ageing and the inception of disease [8, 9]. However, due to their effective redox-active radical-scavenging capabilities, gold, silver, and selenium nanoparticles have been shown to reduce oxidative stress and free radicals [10–12]. By preventing, postponing, or impeding the oxidation of biomolecules, antioxidants regulate oxidative processes [13, 14].

Furthermore, the significant antioxidant properties of some nanomaterials are creating an exciting possibility for developing new regimens with more focused and effective actions. Many natural compounds from medicinal plants have already demonstrated effects against germs, microbes, malignant cells, and neurological diseases. In addition to being environmentally friendly, including plants in a biosynthetic process may improve the biological characteristics of nanoparticles (NPs) [15]. Grown throughout the world as a major oilseed crop, sunflower (*Helianthus annuus*) releases high-quality oil and dietary fibre that are vital to human well-being. This plant belongs to the genus *Helianthus* and family Asteraceae, and it is a short-season species with over 70 species identified globally. The term "sunflower" comes from the plant's size and sun-like appearance [16], and the majority of its products have been sold as animal feed or for cooking [17, 18].

Sunflower oil is now widely acknowledged as a significant source of high-quality edible oil that is used in cooking [19, 20]. Growing sunflowers may be more competitive than growing other crops like maize, soybeans, and sorghum in some nations, such as South Africa and India [21, 22]. This is because decoctions of *H. annuus* leaves, seeds, and flowers are commonly used in the treatment of inflammatory conditions, fever, gastrointestinal disorders, ulcers, skin infections, and microbial infections. The leaves contain lots of bioactive compounds, such as phenolics and flavonoids, which enhance antimicrobial, antioxidant, and anti-inflammatory properties [23]. Unlike some medicinal plants with limited geographical distribution, *H. annuus* can be cultivated across diverse agro-ecological zones with minimal environmental requirements. Additionally, high biomass yield ensures consistency in phytochemical supply. Generally, the leaves

are widely cultivated, non-endangered, and economically accessible, making them a sustainable raw material for large-scale nanoparticle production [24, 25].

While silver nanoparticle synthesis using *Helianthus annuus* from different parts of the plant such as flowers, seeds and leaves has been previously reported [26, 27], limited information exists on the use of methanolic and ethyl acetate leaf extracts and their influence on both antibacterial and antioxidant activities. This study addresses this gap by demonstrating solvent-dependent biosynthesis of AgNPs with dual antimicrobial and antioxidant functionality, thereby extending earlier work beyond nanoparticle formation to bioactivity enhancement.

2 Materials and methods

2.1 Collection of plant materials

Fresh leaves of *Helianthus annuus* were collected from Ajayi Crowther University, Oyo, Nigeria, with a latitude *7° 50' 56" North; longitude. 3° 56' 53" East.*). The leaves of *Helianthus annuus* were authenticated by Mr Esimekhuai Donatus, a Botanist and Taxonomist at the herbarium unit of the University of Ibadan. The voucher specimen was deposited at the University Herbarium with ID UIH-23720. *Helianthus annuus* was used in this study as a choice plant due to its abundant availability, easy accessibility, low-cost, eco-friendly and high sustainability. To get rid of dust and debris, 100 g of recently harvested *Helianthus annuus* leaves were judiciously cleaned with distilled water (DW). After four weeks of air drying in the dimness at 35 °C and 44.6% relative humidity, healthy leaves showing no signs of damage were ground into a powder using a mortar and pestle. The crushed plants were then weighed [28].

2.2 Preparation of methanol and ethyl acetate extract

The powdered *Helianthus annuus* (50 g) sample was weighed and soaked in 250 ml of ethyl acetate (EaHa) and methanol (MHa) in a 500 ml flask and stirred for 5 min. The flasks were left open for evaporation to occur and allowed to soak for three days. Whatman's (No. 1) filter paper was used to separate the liquid portion from the shaft. A dry residue was obtained by concentrating the filtrate with a rotary evaporator and drying it at 45 °C on a water bath. This was kept in a desiccator until it was needed [29].

2.3 Preliminary phytochemical analysis of methanol and ethyl acetate extract

The Mikhailova et al. [30] method was used to determine the quantitative phytochemical analysis. The phytochemical tests of the EaHa and MHa were done to identify if saponins, tannins, flavonoids, cardiac glycosides, anthraquinones, steroids, terpenoids, alkaloids, and phenols were present in the leaf extract.

2.3.1 Test for alkaloids

After pipetting 3 millilitres of the extract into a test tube and adding 1 millilitre of 1% HCl, the extract was heated in a water bath for 20 min before being allowed to cool. Mayer's reagent (0.5 mL) was then added, and the alkaloid was determined by the appearance of a creamy white colour.

2.3.2 Test for flavonoids

Three millilitres of the extract were pipetted into a test tube, to which ten millilitres of distilled water were added. One millilitre of 10% NaOH was then added. The mixture's colour changing to yellow signifies a favourable outcome.

2.3.3 Test for saponin: (Frothing test)

Three millilitres of the extract was pipetted into a test tube, to which 2 ml of distilled water was added. It was then shaken vigorously to see if there was any residual frothing movement.

Three millilitres of the extract was pipetted into a test tube, to which 2 ml of distilled water was added. It was then shaken vigorously to see if there was any residual frothing movement.

2.3.4 Test for steroids

Concentrated H_2SO_4 was added to 1 mL of the extracted leaves in drops and a red colouration showed the occurrence of steroids.

2.3.5 Test for tannins

Three drops of 1% ferric chloride were added to 2 mL of the extract in a test tube, after being boiled in a water bath for 20 min and cooled. A bluish precipitate revealed that tannin was present.

2.4 Microbial cultures for antibacterial assays

Test pathogens, such as *Staphylococcus epidermidis*, *Bacillus subtilis*, *Escherichia coli*, and *Klebsiella pneumonia*, originally isolated from ready-to-eat foods, were used as test pathogens in this study. They were isolated and kept on agar slants, and then stored in a refrigerator for later use.

2.5 Synthesis of silver nanoparticles using *Helianthus annuus*

The synthesis of Silver nanoparticles (AgNPs) using Ethyl acetate *Helianthus annuus* (EaHa) leaves extract and Methanol *Helianthus annuus* (MHa) leaves extract was done using the improved method of Castillo-Henríquez et al. [31]. In a reaction process, 90 mL of 5 mM silver nitrate solution was mixed with 10 mL of the extracts of EaHa and MHa separately at pH 8. The pH was adjusted using sulfuric acid and sodium hydroxide solutions drop by drop. After five minutes of heating the mixture at 90 °C, a sudden colour shift from light green to dark yellowish brown solution, which signalled the synthesis of silver nanoparticles and confirmed that the reduction of Ag^+ to Ag^0 was obtained. It was purified by centrifuging the resulting solution of silver nanoparticles repeatedly for 15 min at 10,000 rpm. In order to allow the particles to settle deeper, repeated centrifugation was carried out, and the supernatant was moved to a dry, clean beaker. The obtained particles were subjected to further characterisation.

2.6 Characterisation of synthesised silver nanoparticles

2.6.1 Visual detection and UV–visible spectrophotometric analysis of AgNPs

The AgNPs produced by utilising EaHa (AgNPEaHa) and MHa (AgNPMHa) were visually inspected for a colour change (light green to dark yellowish brown), signifying the

bioreduction to silver nanoparticles, and were monitored using a UV-visible spectrophotometer (UV-752 Shimadzu Model, USA), at a resolution of 0.5 nm. Four millilitres of the AgNPs were transferred into a quartz cuvette, and their absorbance was read at a wavelength ranging from 650 nm with a bandwidth of 2.0 nm [32]. The spectrum data recorded were then plotted.

2.6.2 Scanning electron microscopy (SEM) of the synthesised AgNPEaHa and AgNPMHa

Using Hitachi scanning electron microscope (Model, s-2600-Tokyo, Japan), the shape and morphology of the AgNPEaHa and AgNPMHa were observed. The biosynthesised samples were freeze-dried and mounted on a coverslip, coated with gold using a coater. An SEM operating in the high vacuum anode with an accelerated voltage of 20 KV was used to capture images of the silver nanoparticles [33]. To form a thin layer of the sample, a tiny amount of the AgNPs was deposited onto a copper grid covered with carbon. The biosynthesised AgNPs were centrifuged at 13,000 rpm for 10 min. The recovered pellet was resuspended in deionised water and centrifuged for 10 min at 13,000 rpm to eliminate any possible organic contamination in the nanoparticles. Lastly, a lyophilizer was used to freeze-dry the pellets.

2.6.3 Transmission electron microscopy (TEM) of the synthesised AgNPEaHa and AgNPMHa

The nanosize and structure of the AgNPs was visualized using the TEM technique (TEM; Philips model CM 200). The operation of the microscope was done at an accelerating voltage of 200 KV with ultra-high resolution of 0.2 nm and magnification of 2,000,000 X. To prepare for the 3 mm grid, 5 uL of the AgNPs solution was placed on carbon-coated copper grids and dried under a mercury lamp before analysis. With the help of image magnifying software, the size of the AgNPs was determined [28, 34].

2.6.4 Energy dispersive X-ray (EDX) and X-ray diffraction analysis of the synthesised AgNPEaHa and AgNPMHa

Using Energy Dispersive X-ray (EDX) (JEOL-JSM-7600 F, US), the elemental makeup of the samples was ascertained. The sample that had been centrifuged was drop-coated on a carbon sheet, and the electron beam was directed onto a specific area on the external of the biosynthesised silver nanoparticles to create a spot-profile mode using a current of 350 μA and voltage of 40.0 kV [33]. Studies of the X-Ray Diffraction (XRD) were performed using X-ray diffractometer (Rigaku D/Max111c, pw1800, China) at 30 kV and 20 mA current with Cu K (I = 1.54 A), which was used to assess the crystalline size and purity of the AgNPs [34]. Using Scherrer's equation, the crystalline size of the produced Ag-NPs was ascertained as follows.

D = crystal size,

λ = X-ray wavelength,

θ = Bragg angle,

β = full width at half maximum of the peak in radians at $D \approx 0.9\lambda/\beta\cos\theta$.

2.6.5 Fourier transform infrared (FT-IR) spectroscopy of the AgNPEaHa and AgNPMHa

The functional groups present on the synthesised AgNPs were characterised by FT-IR spectroscopy. Transparent sample discs were prepared by encapsulating 2 mg of the nanoparticles in a 100 mg KBr pellet. The pelleted samples were characterised by Fourier

transform infrared (FT-IR) spectroscopy over a wavelength range of 350 to 4400 cm^{-1}. The FT-IR spectrum was recorded using a Nicolet iS10 FT-IR Spectrophotometer in China [35].

2.7 Antibacterial potential of the AgNPEaHa and AgNPMHa

The antibacterial activity of the AgNPs was tested against a panel of pathogenic bacterial species, including *Escherichia coli*, *Staphylococcus aureus*, *Pseudomonas* spp., *Klebsiella* spp., and *Staphylococcus epidermis* using the agar well diffusion method. For the assay, Mueller-Hinton agar (MHA) was sterilised by autoclaving for 15 min at 121 °C. The standardized test organisms inoculum was swabbed onto a sterile MHA surface in individual Petri dishes after it had solidified, and the plates were left to dry. Seven steady wells were punctured into the agar with a 4 mm conventional cork borer. Each agar well was treated with the introduction of 5 ug/mL of AgNPEaHa and AgNPMHa. The positive control (12.5 ug/mL of chloramphenicol antibiotic disc) was placed on the sixth well to test against each of the 5 test pathogens while the seventh well was filled with silver nitrate solution (negative control). Following a 24-hour incubation period at 37 °C, the plates were assessed for areas where growth was inhibited. Except for the wells, the clear zones were measured and noted [36, 37]. Three replicates were performed for statistical analysis.

2.8 Antioxidant assay

2.8.1 Determination of reducing power of the AgNPEaHa and AgNPMHa

The silver nanoparticles-reducing power was measured by applying the Adebayo-Tayo et al. [35] method. To 0.75 mL of phosphate buffer (pH 6.6) and 1% of potassium ferricyanide, 200–400 ug of AgNPEa and AgM were added. After 20 min at 50 °C, the mixture was combined with 10% 75 mL trichloroacetic acid, and it was spun for 10 min at 3000 rpm. Furthermore, ferric chloride (0.1%, 0.1 mL) and 1.5 mL of distilled water were included. The absorbance was read at 700 nm after 10 min incubation using ascorbic acid as a standard.

$$\%Antioxidant\,activity = \frac{Control\,OD - Experimental\,OD}{Control\,OD} \times 100$$

where, Control OD = sample's absorption without Ag NPs, Experimental OD = sample's absorption with AgNPs.

2.8.2 Total antioxidant activity of the AgNPEaHa and AgNPMHa

Using the Adebayo-Tayo et al. [35] approach, the total antioxidant potential of AgNPs was measured by adding 1.235 g of ammonium molybdate (4 M), 0.6 M sulfuric acid (45 mL), and 0.0042 g of sodium sulphate to 250 mL of distilled water. After 15 min, two different concentrations (200 and 400 µg) of the AgNPs were mixed with 0.1 mL of total antioxidant capacity, and the absorbance was measured at 695 nm. The reference was ascorbic acid.

$$\%Antioxidant\,activity = \frac{Control\,OD - Experimental\,OD}{ControlOD} \times 100$$

where, Control OD = sample's absorption without AgNPs, Experimental OD= sample's absorption with AgNPs.

2.8.3 Hydrogen peroxide scavenging of the AgNPEaHa and AgNPMHa

Hydrogen peroxide scavenging assay of AgNPs was done using Hydrogen peroxide analysis [38]. Hydrogen peroxide solution (10 mM) was produced in 0.1 M phosphate-buffered saline (pH 7.4). AgNPs (1 ml) of varied concentrations (200 and 400 ug) were hurriedly combined with 2 mL of Hydrogen peroxide solution. After 10 min of incubation at 30 °C, absorbance at 230 nm was read using a UV spectrophotometer against a mixture that lacks hydrogen peroxide, which is used as a blank. Ascorbic acid was used as a standard. The percentage of Hydrogen peroxide was calculated using the formula:

$$Percentage\,of\,scavenging = \frac{Absorbance\,of\,control - Absorbance\,of\,sample}{Absorbance\,of\,control} \times 100$$

2.8.4 Statistical analysis

The data are presented as the means of three replicates ± standard deviations. The results were subjected to analysis of variance (ANOVA), and the differences between means were considered significant at a p-value < 0.05.

3 Results and discussion

3.1 Phytochemical screening

There has been a recent revolution in the use of medicinal plant materials for synthesising nanoparticles, which could offer an alternative to antibiotics [38]. Qualitative phytochemical screening revealed the presence of alkaloids, flavonoids, saponins, tannins and steroids. Saponin and terpenoids are strongly positive; tannins, flavonoids, anthraquinones, steroids and alkaloids are positive. Cardiac glucosides are completely absent in EaHa and MHa, while phenol is only absent in the EaHa leaf extract (Table 1). This discovery is consistent with the findings of Akintola et al. [39] and Ojo et al., [40], who noted the absence of phenol and glucoside in the ethanol extract of *Carica papaya* and *Mangifera indica*. All the identified phytochemicals have both industrial and medicinal significance. For instance, saponin is known for its medicinal use as an antioxidant, anticancer agent, treatment of hypercholesterolemia and hyperglycaemia. Tannin, as documented by Batiha et al. [41], demonstrates antiviral, antibacterial, and antitumor

Table 1 The physicochemical analysis of EaHa and MHa leaves extract

S/*N*	Phytochemical parameters	Extracts	
		EaHa	MHa
1	Saponins	++ve	++ve
2	Tannins	+ve	+ve
3	Flavonoids	+ve	+ve
4	Cardiac glucosides	-ve	-ve
5	Anthraquinones	+ve	+ve
6	Steroids	+ve	+ve
7	Terpenoids	++ve	++ve
8	Alkaloids	+ve	+ve
9	Phenol	-ve	+ve

EaHa Ethyl acetate of *Helianthus annuus*, *MHa* Methanol extract of *Helianthus annuus*,*+ve* Present, *++ve* Abundantly, *-ve* absent

Fig. 1 Visual observation of the biosynthesis of Silver Nitrate to Silver nanoparticle (Visual inspection of colour change). **A** Leaves extract, **B** Silver Nitrate Solution, **C** Synthesized leaf extract

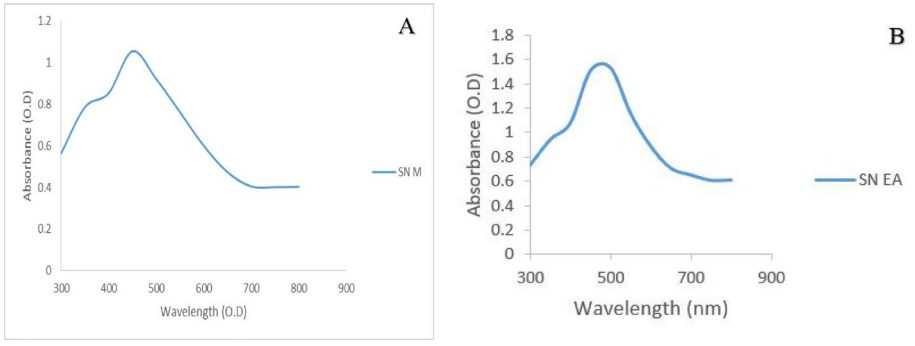

Fig. 2 UV-visible absorption spectra of synthesized **A** AgNPMHa and **B** AgNPEaHa

properties. Research by Barnabas [42] indicated that specific tannins can selectively inhibit HIV replication. Flavonoids possess an innate ability to alter the body's response to allergies, viruses, and carcinogens, displaying activities against allergies, inflammation, microbes, and cancer. Alkaloids have the potential to address severe conditions like heart failure, cancer, and high blood pressure, as stated by Snigdha et al. [43].

3.2 Visual inspection

Observation of a colour variation during nanoparticle formation was previously noted. After adding the leaf extracts of *Helianthus annuus* (methanolic and ethyl acetate) to the silver solution for 20 min, the solution's colour changed from light green to dark yellowish brown, indicating the formation of silver nanoparticles due to the conversion of AG^{+} to Ag^{0}, as shown in Fig. 1. The colour stabilised after 20 min at pH 8 and 90 °C, which is a characteristic sign of surface plasmon resonance (SPR) in the synthesised silver nanoparticles. Numerous previous studies have documented a change in the hue of the solution as an indication of nanoparticle formation from various plant sources [28, 35]. This change results from the reduction of silver ions and the excitation of surface plasmon vibrations, which are characteristic of silver [44, 45].

UV-Visible Spectroscopy Using UV-VIS spectroscopy, the conversion of Ag+ into Ag particles was further verified. The absorbance peak of the silver nanoparticle generated in the reaction media is located at 450 nm for AgNPMHa and 500 nm for AgNPEaHa, suggesting bioreduction of silver nitrate into silver nanoparticles (Figs. 2A and B). The spectra showed no additional peaks. UV-vis spectroscopy is a beneficial and trustworthy

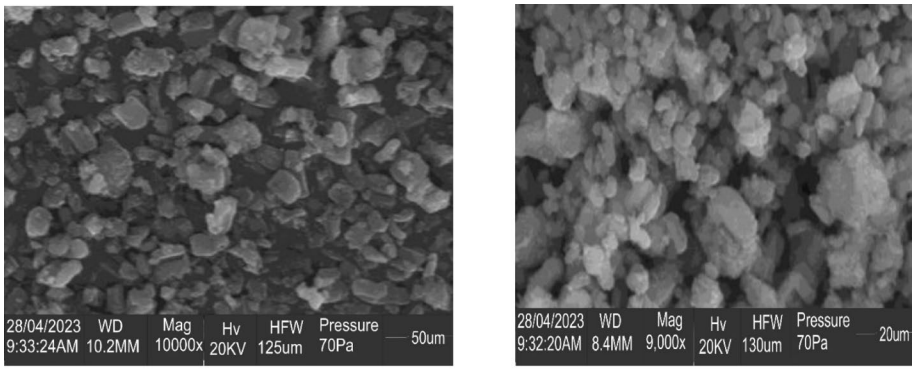

Fig. 3 **a** The SEM of AgNPMHa. **b** The SEM of AgNPEaHa

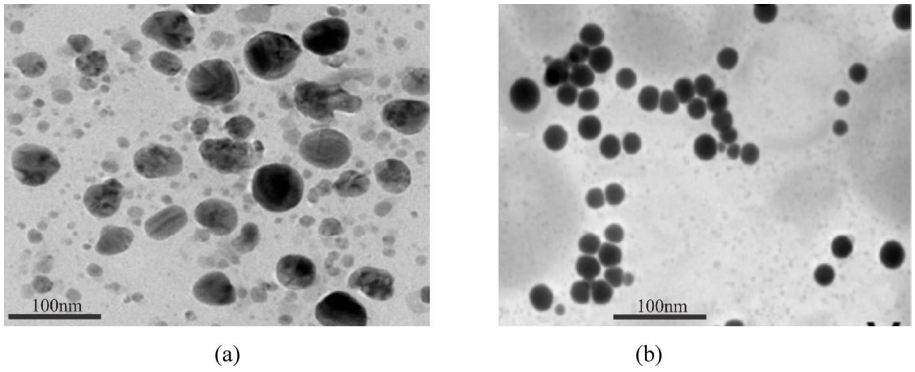

Fig. 4 **a** The TEM of AgNPMHa. **b** The TEM of AgNPEaHa

method for the preliminary characterisation of produced nanoparticles [32]. UV-vis spectrum for silver nanoparticles is mostly within the range of 400–600 nm, which provides a unique optical property resulting from the significant interaction with specific light wavelengths [33]. Oladipo et al. [46] reported a UV-vis spectrum for silver nanoparticles synthesised from *A. conyzoides* with a maximum absorbance of 490.0 nm. Also, Chandraker et al. [47] recorded a salient SPR peak of 440 nm using *Sonchus arvensis* leaf extract. This is a characteristic attribute of silver, which is used to corroborate the existence of AgNPs, as reported previously by Ahmeda et al. [48].

SEM and TEM of AgNPEaHa and AgNPMHa Numerous particle diameters, distributions, nanomaterial forms, and the surface morphology of produced AgNPMHa and AgNPEaHa at the nanoscale were detected using the SEM (Fig. 3a and b) while the particle size distribution using TEM is shown in Fig. 4a and b. The data revealed that silver nanoparticles were agglomerated and had variable shapes, mostly spherical ones. This result is due to the extract's capping agents, which act as stabilisers or binding molecules to give colloidal stability. Some aggregations that were observed are associated with the high surface energy of the nanoscale. The Tem revealed a spherical shape having about sizes of 26.8 ± 9.4 nm for AgNPMHa and 22.3 ± 6.8 nm for AgNPEaHa. The observed fluctuations in the AgNPs size are likely due to divergent nucleation and growth processes driven by parameters such as temperature and reaction [49]. This connects with the findings of Agbaje et al. [50], who noted that the produced nanoparticles were spherical particles within the diameter range of 45–90 nm. In a study by Alahmad et al. [51],

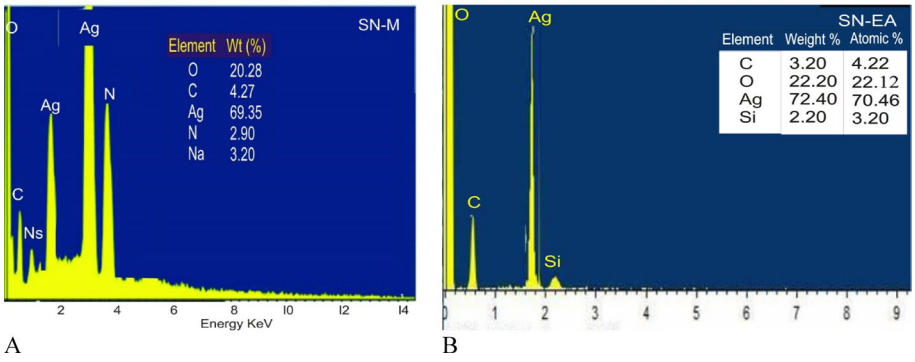

Fig. 5 EDX analysis of synthesized **A** AgNPEaHa and **B** AgNPMHa

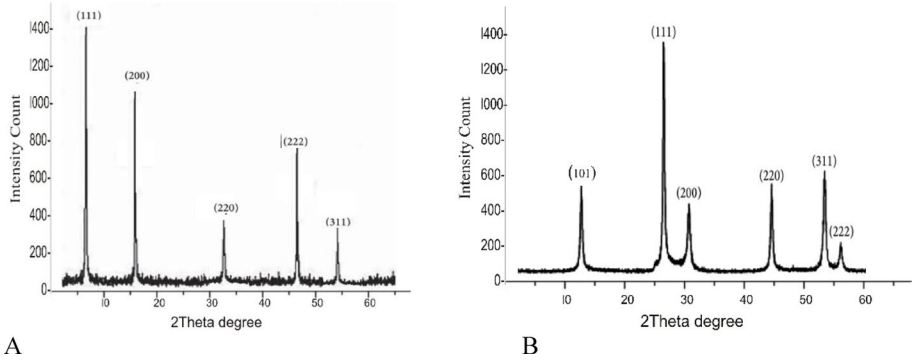

Fig. 6 X-ray diffraction **A** AgNPEaHa and **B** AgNPMHa

it was noted that the biosynthesised AgNPs were within the size range of 15–40 nm. The TEM was done to explore the morphology and size distribution of the AgNPs. Figures 4a and b shows that AgNPMHa and AgNPEaHa are mostly spherical and relatively uniform shape with varied sizes which is in agreement with the UV-vis spectra. Particles were well dispersed and tends to form small agglomerates due to antiparticles and presence of residual phytochemicals for the plant extracts. A similar result was reported by Chandraker et al. [52].

3.3 Energy dispersive X-ray (EDX) and X-ray diffraction analysis (XRD) of AgNPs

Figure 5A and B demonstrate the EDX analysis of the synthesised AgNPs with *H. annuus* extract. A strong silver signal was identified, signifying high purity of the AgNPs obtained through the SPR. The incidence of weak signals for silicon, carbon, and oxygen may be ascribed to the diverse precipitate in the extract. Quantitative analysis using EDX revealed a silver content of 69.35% in AgNPMHa and 72.40% in AgNPEaHa. The spectrum also showed the presence of oxygen, carbon, nitrogen and sodium at 20.28%, 4.27%, 2.90%, and 3.20% in AgNPMHa, while the weight (%) for AgNPEaHa includes 22.20%, 3.20%, and 7.11%, respectively. The application of XRD is to identify phases and characterise the crystal arrangement of nanoparticles [53]. The AgNPs' crystalline nature was validated by X-ray diffraction investigations, as shown in Figs. 6 A and B. The XRD analysis for the biosynthesised AgNPs indicated five diffraction peaks which can be indexed to (111), (200), (220), (222), and (311) for AgNPEaHa and six diffraction peaks (101), (111), (200), (220), (311), and (222) for AgNPMHa, in the whole spectrum

of 2θ values ranging from 10 to 60. Accordingly, XRD may be used to analyse the structural characteristics of a variety of materials, including glasses, polymers, biomolecules, superconductors, inorganic catalysts, and more [53]. During the surveillance of the EDX analysis, the indication of a conspicuous silver signal was detected, and it was as a result of the surface plasmon resonance, demonstrating that the AgNPs obtained were of high purity. The presence of a different precipitate in the extract may clarify the weak signal detected from sodium, carbon, and nitrogen. This aligns with the findings of Miglani and Tani-ishii [54], who similarly observed strong signals from silver atoms in silver nanoparticles.

3.4 Fourier transform infrared spectroscopy (FT-IR) of AgNPEaHa and AgNPMHa

The functional categories involved in the dual processes of the Ag^{+} ion bioreduction and nanoparticle capping were identified via FT-IR spectroscopy, as shown in Figs. 7a and b. The FTIR spectra were produced in the 500–4000 cm^{-1} range, suggesting the presence of a capping agent with the nanoparticle. The bands at 3425.69 and 3441.12 cm^{-1} were found to agree with the O-H and N-H stretching vibration peaks of phenols from

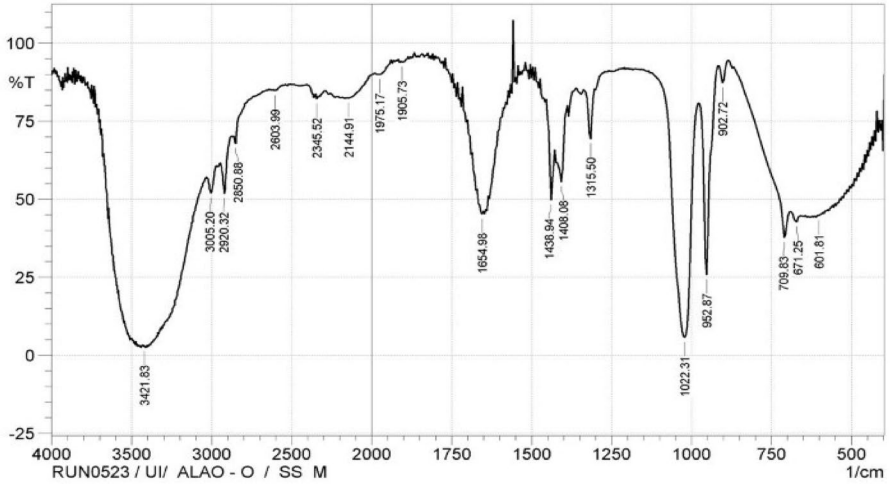

(a)

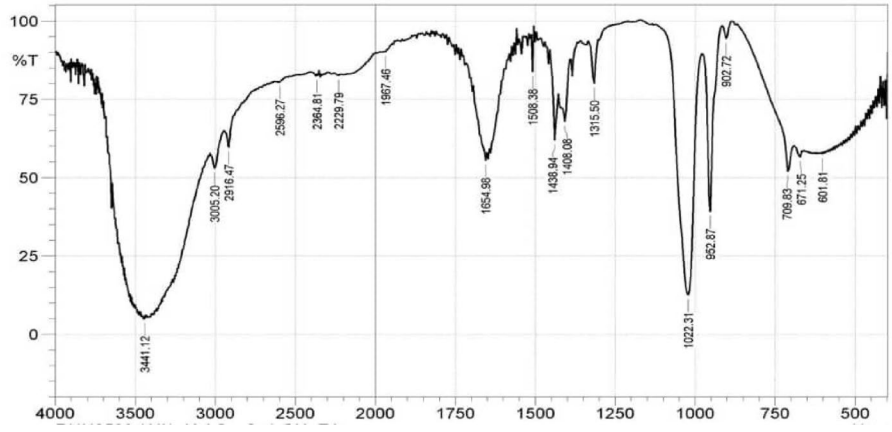

(b)

Fig. 7 **a** FTIR Spectrum of synthesized AgNPs using Methanolic *H. annuus* extract. **b** FTIR spectrum of synthesised AgNPs using Ethyl acetate *H.annuus* extract

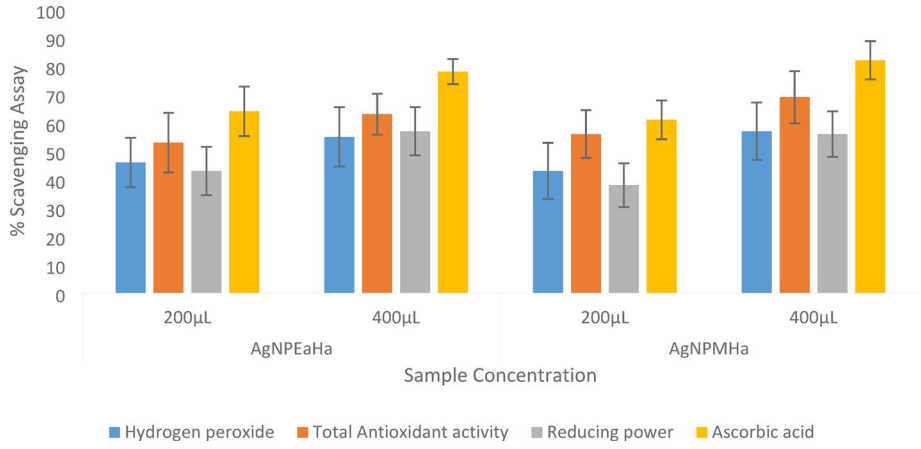

Fig. 8 Antioxidant potential of the synthesized AgNPs using Ethyl acetate *H.annuus* extract

the secondary amine for both the AgNPEaHa and AgNPMHa, respectively. Bands at 2916.47 and 2384.1 cm^{-1} for AgNPEaHa and 2596.27–2229.79 AgNPMHa arising from C – H stretching of aromatic compounds, alcohol/phenol. The bands at 1647.26 cm^{-1} and 1654.98 cm^{-1} in the spectrum correspond to Ester and –C = C-, distinguishing amino acids containing NH_2 groups. The bands at 1508.38 cm^{-1} in the spectra coincide with C-N and C-C stretching, denoting the existence of proteins. The peak at 1139.04–1022.31 cm^{-1} can be attributed to C-OH of the phenols, bolstering the reduction of Ag^+ into Ag^0 through the sharing of polyphenols such as flavonoids, saponins and triterpenoids. The peak at 601 cm^{-1} may correspond to the formation of Ag-O, which confirms the formation of AgNPs. According to the results of the FTIR analysis, polyphenolic groups may act as capping and reducing agents, which would cause silver nanoparticles to develop in the medium [32]. According to Rattana et al. [52, 55], these results are in line with those found for other plant sources. Narrow peaks indicate that the generated nanoparticles were quite small, ranging in size from 1 to 100 nm [56].

3.5 Antioxidant potential of AgNPEaHa and AgNPMHa

Three distinct assays: hydrogen peroxide, reducing power, and total antioxidant are used in Fig. 8 to illustrate the antioxidant capability of AgNPEaHa and AgNPMHa. When 200 µL of AgNPEaHa was used, the hydrogen peroxide assay, total antioxidant assay and reducing power assay showed values of 46 ± 8.72%, 53 ± 10.54%, and 43 ± 8.54%, respectively. The values for the assays at 400 µL were 57.03 ± 5.17%, 80.62 ± 7.21%, and 89 ± 6.38%, respectively. Remarkably, the total antioxidant assay displayed the uppermost scavenging activity at 200 µL, while the reducing power assay recorded the least. Interestingly, at 400 µL, reducing power demonstrated the highest scavenging assay. However, ascorbic acid displayed a higher inhibition activity of 64 ± 7.21%, and 78 ± 7.21% at 200 µL, while at 400 µL, the scavenging activity were 61 ± 7.21% and 82 ± 7.21% for both AgNPs.

The antioxidant potential of the *Helianthus annuus* was recognised because of its contents of chlorogenic acid and many other phytochemical constituents. Since silver is a necessary component of antioxidant enzymes, its role in plants is mostly related to its antibacterial qualities. They play crucial functions in scavenging free radicals, which are unstable substances that can harm cells through oxidative damage, by shielding the cells

Table 2 Antibacterial activity of AgNPs using *H. annuus* in methanol

Samples	Test Pathogen (mm)				
	Escherichia coli	***Staphylococcus aureus***	***Pseudomonas aeruginosa***	***Staphylococcus epididermis***	***Klebsiella pneumoniae***
AgNPEaHa	22.00 ± 4.12	16.00 ± 4.02	00.00	12.00 ± 2.03	00.00
AgNPMHa	10.30 ± 3.06	00.00	00.00	00.00	12.00 ± 1.06
Negative control	06 ± 0.06	0.00	02.00 ± 0.04	03 ± 0.09	0.00
Positive control	27.00 ± 2.12	21.00 ± 3.02	16.00 ± 1.47	19.00 ± 1.03	21.00 ± 2.91

from oxidative damage [57]. Previously reported research findings showed a similar free radical scavenging activity as indicated by AgNPEaHa and AgNPMHa [52, 57]. Adherence of the functional group to the surface of the NPs resulted from the free radical scavenging activity [52].

3.6 Antibacterial activity of AgNPEaHa and AgNPMHa

The antimicrobial properties of the AgNPs were evaluated against foodborne pathogens is shown in Table 2. The AgNPEaHa and AgNPMHa showed a strong antibacterial effect against *Escherichia coli* (22.00 ± 4.12 mm), followed by *Staphylococcus aureus* (16.00 ± 4.02 mm) and *Staphylococcus epidermidis* (12.00 ± 1.06 mm), while *Pseudomonas* spp. and *Klebsiella* spp. showed no inhibition. Comparing the antibacterial activity of AgNPEaHa and AgNPMHa with the positive control (chloramphenicol) revealed that the antibiotic had higher inhibition (16 ± 1.07–27.00 ± 2.12 mm) against the five pathogens, while the silver nitrate solution (negative control) had a very low inhibitionPrevious research observed a general rise in the antibacterial activity of AgNPs of blossom leaves and stems of *Zinnia elegans* extracts [54, 58]. Similar to these results, synthesised nanoparticles have been shown to create zones of inhibition against pathogens like *S. aureus*, *S. epidermis*, and *P. aeruginosa* [59]. AgNPs act on bacterial strains, either damaging the cell by binding to the bacterial cell membrane or increasing permeability, resulting in cell death through leakage of cellular material [60]. Other attributes for the antimicrobial potential of silver nanoparticles include membrane permeability alteration, the reactive oxygen species formation, the release of lipopolysaccharides from the membrane, and the breakdown of the membrane potential [60]. Silver has already proven to be a promising drug in the fight against antibiotic resistance due to its multitargeted activity. It has been demonstrated that AgNPs alter the structure of bacterial cell membranes, which can be utilised to make bacteria more susceptible to antibiotics [57].

3.7 Novelty statement

This study reports the successful green synthesis of silver nanoparticles using ethyl acetate and methanol leaf extracts of *Helianthus annuus* L. for the first time. The novelty of this pioneering research proved exceptional effectiveness, with unusually high elemental silver content (exceeding 69.35%), and demonstrated antioxidant activity in a dose-dependent manner. This finding establishes sunflower leaves, often known as a weed, as a potent, cost-effective, and eco-friendly biomaterial for generating AgNPs with promising applications.

3.8 Limitations of the study

This study is limited by its reliance on in vitro assays, as no in vivo experiments were conducted to validate the safety, efficacy, or biological behaviour of the synthesised silver nanoparticles. The absence of cytotoxicity and biocompatibility assessments on mammalian cell lines restricts their potential biomedical application. In addition, the mechanism of antimicrobial action was not experimentally elucidated. The study also lacked advanced colloidal stability analyses, such as zeta potential and dynamic light scattering, as well as long-term stability and reproducibility assessments of the green synthesis process. Future research should therefore focus on comprehensive toxicity and in vivo studies, detailed mechanistic investigations, comparative evaluation with crude plant extracts, and optimisation of synthesis conditions to improve nanoparticle stability, scalability, and applicability in biomedical and food safety contexts.

4 Conclusion

This present finding has revealed the effectiveness of biosynthesised silver nanoparticles of methanolic and ethyl acetate *H. annuus* leaf extracts against bacterial pathogens and oxidative stress. The nanoparticles were spherical, and acted as an exceptional capping and stabilising agent for the speedy and eco-friendly silver nanoparticles. The absorbance peak at 450 nm for AgNPEaHa and 500 nm for AgNpMHa indicated a silver characteristic band. Hydroxyl, alcohol, phosphate, and amine were the functional groups in both AgMPEaHa and AgNpMHa. This finding aligns with Sustainable Development Goals 3 (Good Health and Well-being), 9 (Industry, Innovation, and Infrastructure), and 13 (Responsible Consumption and Production).

Acknowledgements
The authors appreciate the laboratory technologists (Mrs U.C. Mbabie and Mr Bello) in the Department of Microbiology and Biotechnology, Ajayi Crowther University, for their support.

Author contributions
R.O. did conceptualization, Methodology, Experiments; R.O., A.A. and O.P. supervise, and writing original draft, R. O., S.A., O.O. and S.N. did methodology, analysis and writing original draft. All authors reviewed the manuscript.

Funding
This research did not receive any funding or grant from any funding agencies, either public or commercial.

Data availability
The datasets generated during and/or analysed during the current study are available from the corresponding author on reasonable request.

Declarations

Ethics approval and consent to participate
Not applicable because the present work does not involve any human or animal study.

Consent for publication
The authors declare no conflict of interest.

Competing interests
The authors declare no competing interests.

Received: 20 November 2025 / Accepted: 2 March 2026
Published online: 11 March 2026

References

1. Zheng JX, Wu Y, Lin ZW, et al. Characteristics of and virulence factors associated with biofilm formation in clinical *Enterococcus faecalis* isolates in China. Front Microbiol. 2017;8:2338–45. https://doi.org/10.3389/fmicb.2017.02338.
2. Karim N, Liu S, Rashwan A, et al. Green synthesis of nanolipo-fibersomes using Nutriose® FB 06 for delphinidin-3-O-sambubioside delivery: characterization, physicochemical properties, and application. Int J Biol Macromol. 2023;247:125839. https://doi.org/10.1016/j.ijbiomac.2023.125839.

3. Xulu JH, Ndongwu T, Ezealisiji KM, et al. The use of medicinal plant-derived metallic nanoparticles in theranostics. Pharm. 2022;14(11):2437. https://doi.org/10.3390/pharmaceutics14112437.
4. Potter PM, Navratilova J, Rogers KR, et al. Transformation of silver nanoparticle consumer products during simulated usage and disposal. Environ Sci Nano. 2019. https://doi.org/10.1039/C8EN00958A.
5. Kindly provide the complete reference details of 5
6. Maitra B, Khatun MH, Ahmed F, et al. Biosynthesis of *Bixa orellana* seed extract mediated silver nanoparticles with moderate antioxidant, antibacterial and antiproliferative activity. Arab J Chem. 2023;16(5):1–15. https://doi.org/10.1016/j.arabjc.2023.104675.
7. Chakraborty S, Rao CV, Das R, et al. Bio-mediated silver nanoparticle synthesis: mechanism and microbial inactivation. Toxicol Environ Chem. 2017;9(3):434–47. https://doi.org/10.1080/02772248.2016.1214271.
8. Phumthum M, Srithi K, Inta A, et al. Ethnomedicinal plant diversity in Thailand. J Ethnopharmacol. 2018;214:90–8. https://doi.org/10.1016/j.jep.2017.12.003.
9. Xu L, Wang YY, Chen CY, et al. Silver nanoparticles: synthesis, medical applications and biosafety. Theranostics. 2020;10(20):8996. https://doi.org/10.7150/thno.45413.
10. Murugan R, Thangaraj P, et al. Comparative evaluation of different extraction methods for antioxidant and anti-inflammatory properties from *Osbeckia parvifolia* Arn.—an in vitro approach. J King Saud Uni Sci. 2014;26(4):267–75. https://doi.org/10.1016/j.jksus.2013.09.006.
11. Guntur SR, Kumar NS, Hegde MM, et al. In vitro studies of the antimicrobial and free-radical scavenging potentials of silver nanoparticles biosynthesized from the extract of *Desmostachya bipinnata*. Anal Chem Insights. 2018;13:1–8. https://doi.org/10.1177/1177390118782877.
12. Ibrahim NH, Awaad AS, Alnafisah RA, et al. In-vitro activity of *Desmostachya bipinnata* (L.) stapf successive extracts against *Helicobacter pylori* clinical isolates. Saudi Pharm. 2018;J26:535–40. https://doi.org/10.1016/j.jsps.2018.02.002.
13. Duman F, Ocsay I, Kup FO, et al. Chamomile flower extract-directed CuO nanoparticle formation for its antioxidant and DNA cleavage properties. Mat Sci Eng. 2016;60:333–8. https://doi.org/10.1016/j.msec.2015.11.052.
14. Üstün EE, Önba SC, Çelik SK, et al. Green synthesis of iron oxide nanoparticles by using *Ficus carica* leaf extract and its antioxidant activity. Bio Res Appl Chem. 2022;12(6):2108–16. https://doi.org/10.33263/BRIAC122.21082116.
15. Kunjan F, Shanmugam R, Govindharaj S, et al. Evaluation of free radical scavenging and antimicrobial activity of *Coleus amboinicus*-mediated iron oxide nanoparticles. Cereus. 2024;16(3):1–10. https://doi.org/10.7759/cureus.55472.
16. Fashogbon RO, Akinade KJ, Emozozo OH, et al. Green synthesis of selenium nanoparticles from *Helianthus annuus* leaf extracts: antioxidant and antimicrobial activities on food borne pathogens. STNANOMAT J 2025. 9(2):3. https://doi.org/10.4314/nano/v9i2.3.
17. Stoikou V, et al. Metal uptake by sunflower (*Helianthus annuus*) irrigated with water polluted with chromiun and nickel. Foods. 2017;6(7):51. https://doi.org/10.3390/foods6070051.
18. Yegorov B, Trupurova T, Sharabaeva E, et al. Prospects of using by-products of sunflower oil production in compound feed industry. J Food Sci Technol. 2019;13:106–13. https://doi.org/10.15673/fst.v13i1.1337.
19. Mukherjee AK, Tripatho S, Mukherjee S, et al. Effect of integrated nutrient management in sunflower (*Helianthus annuus* L.) on alluvial soil. Cur Sci. 2019;117(8):1364.
20. Jinadasa B, Bockstaele FV, Cvejic JH, et al. Current trends and next generation of future edible oils. Future foods. 2022;203–31. https://doi.org/10.1016/B978-0-323-91001-9.00005-0.
21. Forleo MB, Nadia P, Alessandro S, et al. The eco-efficiency of rapeseed and sunflower cultivation in Italy. Joining environmental and economic assessment. J Cl Prod. 2018;172:3138–53. https://doi.org/10.1016/j.jclepro.2017.11.094.
22. Laguna O, Barakat A, Alhamada H, et al. Production of proteins and phenolic compounds enriched fractions from rapeseed and sunflower meals by dry fractionation processes. Ind Crops Prod. 2018;118:160–72. https://doi.org/10.1016/j.indcrop.2018.03.045.
23. Antonopoulou G, Vayenas D, et al. Ethanol and hydrogen production from sunflower straw: the effect of pretreatment on the whole slurry fermentation. Biochem Eng J. 2016;116:65–74. https://doi.org/10.1016/j.bej.2016.06.014.
24. Ebrahimian E, Seyyedi SM, et al. Seed yield and oil quality of sunflower, safflower, and sesame under different levels of irrigation water availability. Agric Water Manag. 2019;218:149–57. https://doi.org/10.1016/j.agwat.2019.03.031.
25. Bashir T, Zahara K, Haider S, et al. Chemistry, pharmacology and ethnomedicinal uses of *Helianthus annuus* (sunflower): a review. Pure App Bio. 2015;4(2):226. https://doi.org/10.19045/bspab.2015.42011.
26. Adeleke BS, Babalola OO. Oilseed crop sunflower (*Helianthus annuus*) as a source of food: nutritional and health benefits. Food Science & Nutrition. 2020;8(9):4666–84. https://doi.org/10.1002/fsn3.1783.
27. Shaheen S, Humma Z, Arooj I, et al. Green synthesis of silver nanoparticles from flowers of *Helianthus annuus* and *Tagetes erecta* and their antibacterial activity against MDR pathogens. RADS Journal of Biological Research & Applied Sciences. 2021;12(2):98–107.
28. Chandraker SK, Lal M, et al. Therapeutic potential of biogenic and optimized silver nanoparticles using *Rubia cordifolia* L. leaf extract. Sci Rep. 2022;12:8831.
29. Fashogbon RO, Akinade KJ, Emozozo O, et al. Green synthesis of selenium nanoparticles from Helianthus annuus lead extracts: antioxidant and antimicrobial activities on foofnorne pathogens. Nano Plus Sci Technol Naonomater. 2025;9(2):27–39.
30. Mikhailova EO. Gold nanoparticles: biosynthesis and potential of biomedical application. J Funct Biomater. 2021;12:70. https://doi.org/10.3390/jfb12040070.
31. Castillo-Henríquez L, Alfaro-Aguilar K, Ugalde-Alvarez J, et al. Green synthesis of gold and silver nanoparticles from plant extracts and their possible applications as antimicrobial agents in the agricultural area. Nanomaterials. 2020. https://doi.org/10.3390/nano10091763.
32. Lal S, Verma R, Chauhan A, et al. Antioxidant, antimicrobial, and photocatalytic activity of green synthesized ZnO-NPs from *Myrica esculenta* fruits extract. Inorg Chem Commun. 2022;141:109518. https://doi.org/10.1016/j.inoche.2022.109518.
33. Kumar L, Navneeta B. Biosynthesis, characterization, and evaluation of antibacterial and photocatalytic dye degradation activities of silver nanoparticles biosynthesized by *Chlorella sorokiniana*. Bio Conv Bioref. 2022;22:1–11. https://doi.org/10.1007/s13399-022-03433-w.

34. Bindhu MR, Umadevi M, Esmail GA, et al. Green synthesis and characterization of silver nanoparticles from *Moringa oleifera* flower and assessment of antimicrobial and sensing properties. J Photochem Photobiol B Biol. 2020;205:111836. https://doi.org/10.1016/j.jphotobiol.2020.111836.
35. Adebayo-Tayo B, Ishola R, et al. Characterization, antioxidant and immunomodulatory potential on exopolysaccharide produced by wild type and mutant *Weissella confusa* strains. Biotechnol Rep (Amst). 2018. https://doi.org/10.1016/j.btre.2018.e00271.
36. Arokiyaraj S, Arasu MV, Vincent S, et al. Rapid green synthesis of silver nanoparticles from *Chrysanthemum indicum* L and its antibacterial and cytotoxic effects: an in vitro study. Int J Nanomed. 2014;9:379–88. https://doi.org/10.2147/IJN.S53546.
37. Fashogbon RO, Aforijiku S, Olusesi TI, et al. Phytochemical and antimicrobial potentials of aquous leaves ectracts of *H. annuus* (sunflower): a natural preservative in food industry. Greener J Agric Sci. 2025;15(1):53–62. https://doi.org/10.15580/gjas.2025.2.062725106.
38. Alshehri AA, Malik MA et al. Phytomediated photo-induced green synthesis of silver nanoparticles using *Matricaria chamomilla* L. and its catalytic activity against Rhodamine B Biomol,2020;10 (12):1604. https://doi.org/10.3390/biom10121604
39. Akintola AO, Kehinde BD, Ayoola PB et al. Antioxidant properties of silver nanoparticles biosynthesized from methanolic leaf extract of *Blighia sapida*. IOP Conference series. Mat Sci Eng, 2020;805. https://doi.org/10.1088/1757-899X/805/1/012004
40. Ojo AB, Adanlawo IG, Ojo OA. Efficacy of saponins from *Helianthus annuus* roots on antihyperglycemic, antiperoxidative and antihyperlipidemic effects in alloxan-induced diabetic rats. Int J Pharmacogn Phytochem Res. 2017;9(1):83–8. https://doi.org/10.25258/ijpapr.v9i1.8046.
41. Batiha GS, Alkazmi LM, Nadwa E, et al. Physostigmine: a plant alkaloid isolated from *Physostigma venenosum*: a review on pharmacokinetics, pharmacological and toxicological activities. J Drug Deliv Ther. 2020;10:187–90. https://doi.org/10.22270/jddt.v10i1-s.3866.
42. Barnabas FO, Wuyep PA, Obela UM, et al. Phytochemical analysis and antimicrobial effects of *Carica papaya* leaf extracts on unrinary tract infections. J Bio Innov. 11(2):350–74. https://doi.org/10.46344/JBINO.2022.v11i02.09.
43. Snigdha S, Mishra R, Gautam N, et al. Phytochemical analysis of papaya leaf extract: screening test. EC Dent Sci. 2019;18(3):485–90.
44. Giri AK, Jena B, Biswal B, et al. Green synthesis and characterization of silver nanoparticles using *Eugenia roxburghii* DC. extract and activity against biofilm-producing bacteria. Sci Rep. 2022;12:8383. https://doi.org/10.1038/s41598-022-12484-y.
45. Gontijo LP. pH effect on the synthesis of different size silver nanoparticles evaluated by DLS and their size-dependent antimicrobial activity. Matéria (Rio de Janeiro). 2020;25:e-12845. https://doi.org/10.1590/S1517-707620200004.1145.
46. Oladipo IC, Ibrahim AI, Ogusana SB, Ogunleke OB, et al. Ageratum conyzoides leaf extract mediated silver nanoparticles: a green study on antimicrobial, anticoagulant and wound healing properties. Nano Plus Sci Tech Nanomater. 2025;9:11–23.
47. Chandraker SD, Ghosh MK, Lal M, Ghorai TK, Shukla R, et al. Colorimetric sensing of Fe3 + and Hg2 + and photocatalytic activity of green synthesized silver nanoparticles from the leaf extract of *Sonchus arvensis* L. New J Chem. 2019. https://doi.org/10.1039/C9NJ01338E.
48. Ahmeda A, Akram Z, Mahdi ZM, et al. Green synthesis and chemical characterization of gold nanoparticle synthesized using *Camellia sinensis* leaf aqueous extract for the treatment of acute myeloid leukemia in comparison to daunorubicin in a leukemic mouse model. Appl Organ Chem. 34. https://doi.org/10.1002/aoc.5290.
49. Luo Q, Su W, Li H, et al. Antibacterial activity and catalytic activity of biosynthesised silver nanoparticles by flavonoids from petals of *Lilium casa blanca*. Micro & Nano Letters. 2018;13:824–8. https://doi.org/10.1049/mnl.2018.0055.
50. Agbaje L, Folarin BJ, Oladejo SM, et al. Characterization, antimicrobial, antioxidant, and anticoagulant activities of silver nanoparticles synthesized from *Petiveria alliacea* L. leaf extract. Prep Biochem Biotechnol. 2018;48(7):646–52. https://doi.org/10.1080/10826068.2018.1479864.
51. Alahmad A, Al-Zereini W, Hijazin, et al. Green synthesis of silver nanoparticles using *Hypericum perforatum* L. aqueous extract with the evaluation of its antibacterial activity against clinical and food pathogens. Pharmaceut. 2022;14(5):1104. https://doi.org/10.3390/pharmaceutics14051104.
52. Chandraker SK, Lal M, et al. DNA-binding, antioxidant, H2O2 sensing and photocatalytic properties of biogenic silver nanoparticles using *Ageratum conyzoides* L. leaf extract. RSC Adv. 2019. https://doi.org/10.1039/C9RA03590G.
53. Dashora A, Rathore K, Raj S, et al. Synthesis of silver nanoparticles employing *Polyalthis longifolia* leaf extract and their in vitro antifungal activity against phytopathogen. Biochem Biophys Rep. 2022. https://doi.org/10.1016/j.bbrep.2022.101320.
54. Miglani S, Tani-ishii N. Biosynthesized selenium nanoparticles: characterization, antimicrobial, and antibiofilm activity against *Enterococcus faecalis*. PeerJ. 2021;30:9. https://doi.org/10.7717/peerj.11653.
55. Rattana S, et al. Antioxidant activities, total phenolic and total flavonoid contents of *Oxyceros horridus* crude extracts. JTT Medical Res. 2020;6:1–10.
56. Alkhulaifi MM, et al. Green synthesis of silver nanoparticles using citrus limon peels and evaluation of their antibacterial and cytotoxic properties. Saudi J Biol Sci. 2020;27(12):3434–41. https://doi.org/10.1016/j.sjbs.2020.09.031.
57. Farahmandfar R, Asnaashari M, Pourshayegan M, et al. Evaluation of antioxidant properties of lemon verbena (*Lippia citriodora*) essential oil and its capacity in sunflower oil stabilization during storage time. Food Sci Nutr. 2018;6(4):983–90.
58. Bharathi D, et al. Biosynthesis of silver nanoparticles using stem bark extracts of *Diospyros montana* and their antioxidant and antibacterial activities. J Nanostruct Chem. 2018;8:83–92. https://doi.org/10.1007/s40097-018-0256-7.
59. Abada E. Review green synthesis of silver nanoparticles by using plant extract and their antimicrobial activity. Saudi J Biol Sci. 2024;31(1):1–10. https://doi.org/10.1016/j.sjbs.2023.103877.
60. Kambale EK. Green synthesis of antimicrobial silver nanoparticles using aqueous leaf extracts from three Congolese plant species (*Brillantaisia patula*, *Crossopteryx febrifuga* and *Senna siamea*). Heliyon. 2020;6:e04493. https://doi.org/10.1016/j.heliyon.2020.e04493.

Publisher's Note